J. Am. Chem. Soc. 1992, 114, 8669-8675

Photoelectron Spectra of Phthalocyanine Thin Films: A Valence Band Theoretical Interpretation

Enrique Orti[†] and Jean-Luc Brédas*[,‡]

Contribution from the Departamento de Química Física, Universitat de València, Dr. Moliner 50, E-46100 Burjassot, Spain, and Service de Chimie des Matériaux Nouveaux et Département des Matériaux et Procédés, Université de Mons-Hainaut, Place du Parc 20, B-7000 Mons, Belgium.

Received February 6, 1992

Abstract: A theoretical investigation of the photoelectron valence band spectra of metal-free phthalocyanine (H_2Pc) thin films is performed using the nonempirical valence effective Hamiltonian (VEH) quantum-chemical method. The results of the VEH band structure calculations are presented in the form of theoretical UPS and XPS simulations and are analyzed by comparison to the electronic structure of the H_2Pc molecule. The theoretical spectra are found to be fully consistent with experimental solid-state synchrotron ($h\nu$ = 100 eV) and XPS spectra. An excellent quantitative agreement between theory and experiment is achieved when comparing the energies of the main peaks. A detailed interpretation of all the photoemission bands constituting the experimental spectra is reported in the light of the VEH predictions.

I. Introduction

Phthalocyanines (Pc's) are among the most stable organic materials undergoing no noticeable degradation in air up to 400–500 °C. This exceptional thermal stability, together with their large chemical versatility, make feasible the obtention of high-quality thin films of a great variety of phthalocyanines by successive sublimation. In this context and using the own words of Robertson, who as early as 1935 performed the first determination of the crystal and molecular structure of phthalocyanines:[1] "It is remarkable that the complex phthalocyanine molecule should be the first organic structure to yield an absolutely direct X-ray analysis which does not even involve any assumptions regarding the existence of discrete atoms in the molecule." These and other unique properties they exhibit have warranted the vast amount of basic and applied research concerning phthalocyanines.[2] Industrially, they have been studied for their use as dyes and pigments and for their electrocatalytic activity and suitability for semiconductor devices.[2-4] More recently, phthalocyanines have been of particular interest in many fields concerning energy conversion (photovoltaic and solar cells),[2,5] electrophotography,[6] photosensitizers,[7] gas sensors,[8] rectifying devices,[9] low dimensional metals,[10] electrochromism,[11] optical data storage,[12] Langmuir–Blodgett (LB) films,[13] liquid crystals,[14] and nonlinear optics.[15]

Most of the applications mentioned above for phthalocyanine-based materials are governed by the electronic structure of the phthalocyanine molecule. It is therefore very important to elucidate this structure in order to understand the electronic and optoelectronic phenomena involved in proposed applications. It is then not surprising that the electronic valence band structure of phthalocyanines has been the subject of numerous experimental and theoretical investigations using very different techniques.[2] Among these techniques, photoelectron spectroscopy has been established as a very powerful tool for probing the electronic structure of molecules and solids, and a large number of photoemission studies has been reported for phthalocyanines. Since in this paper we are especially interested in these studies, we briefly review them below.

As early as 1963, Vilesov et al.[16] reported the first photoemission study on metal-free (H_2Pc) and a number of metal phthalocyanines (MPc's) using a photon energy of 10.6 eV. This study was reexamined in 1968 by Schechtman and Spicer[17] using the same photon energy. In 1973, Pong and Smith[18] obtained the He I ($h\nu$ = 21.2 eV) photoelectron spectrum of CuPc, and, in 1976, Kawai et al.[19] employed X-ray photoelectron spectroscopy (XPS) and ultraviolet photoelectron spectroscopy (UPS) techniques to study the chemisorption of various molecules on H_2Pc and several MPc's (especially FePc). We note that prior to these pioneering photoemission works Kearns and Calvin[20] and Pope,[21] knowing the importance of the ionization potential as a parameter governing the electronic and electrical behavior of organic solids, determined the surface ionization potentials of a number of phthalocyanines.

---

* Author to whom correspondence should be addressed.

[†] Universitat de València.

[‡] Université de Mons-Hainaut.

(1) Robertson, J. M. *J. Chem. Soc.* **1935**, 615. Robertson, J. M. *Ibid.* **1936**, 1195. Linstead, R. P.; Robertson, J. M. *Ibid.* **1936**, 1736. Robertson, J. M.; Woodward, I. J. *Ibid.* **1937**, 219.

(2) See, for example: Simon, J.; André, J.-J. *Molecular Semiconductors*; Springer: Berlin, 1985; Chapter III.

(3) Lever, A. B. P.; Hempstead, M. R.; Leznoff, C. C.; Lin, W.; Melnik, M.; Nevin, W. A.; Seymour, P. *Pure Appl. Chem.* **1986**, *58*, 1467. Lever, A. B. P. *Adv. Inorg. Chem. Radiochem.* **1965**, *7*, 27.

(4) Meier, H. *Organic Semiconductors*; Verlag Chemie: Weinheim, 1974. Pope, M.; Swenberg, C. E. *Electronic Processes in Organic Crystals*; Clarendon: Oxford, 1982.

(5) Loutfy, R. O.; Sharp, J. H. *J. Chem. Phys.* **1979**, *71*, 1211. Tang, C. W. *Appl. Phys. Lett.* **1986**, *48*, 183.

(6) Loutfy, R. O.; Hor, A. M.; Hsiao, C. K.; Baranyi, G.; Kazmaier, P. *Pure Appl. Chem.* **1988**, *60*, 1047.

(7) Kato, M.; Nishioka, Y.; Kaifu, K.; Kawamura, K.; Ohno, S. *Appl. Phys. Lett.* **1985**, *46*, 196.

(8) Collins, R. A.; Mohamed, K. A. *J. Phys. D* **1988**, *21*, 154. Temofonte, T. A.; Schoch, K. F. *J. Appl. Phys.* **1989**, *65*, 1350. Sadaoka, Y.; Jones, T. A.; Göpel, W. *Sensors Actuators B* **1990**, *1*, 148.

(9) Abe, K.; Sato, H.; Kimura, T.; Ohkatsu, Y.; Kusano, T. *Makromol. Chem.* **1989**, *190*, 2693.

(10) For recent reviews, see: (a) Marks, T. J. *Science* **1985**, *227*, 881. Marks, T. J. *Angew. Chem., Int. Ed. Engl.* **1990**, *29*, 857. (b) Hoffman, B. M.; Ibers, J. A. *Acc. Chem. Res.* **1983**, *16*, 15. Palmer, S. M.; Stanton, J. L.; Martinsen, J.; Ogawa, M. Y.; Hener, W. B.; Van Wallendael, S. E.; Hoffman, B. M.; Ibers, J. A. *Mol. Cryst. Liq. Cryst.* **1985**, *125*, 1. (c) Hanack, M.; Datz, A.; Fay, R.; Fischer, K.; Keppeler, U.; Koch, J.; Metz, J.; Mezger, M.; Schneider, O.; Schulze, H. J. In *Handbook of Conducting Polymers*; Skotheim, T. A., Ed.; Marcel Dekker: New York, 1986; Vol. 1, Chapter 5, p 133.

(11) Corker, G.; Grant, B.; Clecak, C. *J. Electrochem. Soc.* **1979**, *126*, 1339. Collins, G. C. S.; Schiffrin, D. J. *Ibid.* **1985**, *132*, 1835. Riou, M.-T.; Clarisse, C. *J. Electroanal. Chem.* **1988**, *249*, 181.

(12) Kuder, J. E. *J. Imag. Sci.* **1988**, *32*, 51.

(13) Roberts, G. G.; Petty, M. C.; Baker, S.; Fowler, M. T.; Thomas, N. J. *Thin Solid Films* **1985**, *132*, 113. Cook, M. J.; Dunn, A. J.; Daniel, M. F.; Hart, R. C. O.; Richardson, R. M.; Roser, S. J. *Ibid.* **1988**, *159*, 395. Palacin, S.; Lesieur, P.; Stefanelli, I.; Barraud, A. *Ibid.* **1988**, *159*, 83.

(14) Van der Pol, J. F.; Neeleman, E.; Zwikker, J. W.; Nolte, R. J. M.; Drenth, W.; Aerts, J.; Visser, R.; Picken, S. J. *Liq. Cryst.* **1989**, *6*, 577. Simon, J.; Sirlin, C. *Pure Appl. Chem.* **1989**, *61*, 1625.

(15) Casstevens, M. K.; Samoc, M.; Pfleger, J.; Prasad, P. N. *J. Chem. Phys.* **1990**, *92*, 2019. Simon, J.; Bassoul, P.; Norvez, S. *New J. Chem.* **1989**, *13*, 13.

(16) Vilesov, F. I.; Zagrubskii, A. A.; Garbuzov, D. F. *Tverd. Tela* **1963**, *5*, 2000; *Sov. Phys. Sol. State* **1964**, *5*, 1460.

(17) Schechtman, B. H.; Spicer, W. E. *Chem. Phys. Lett.* **1968**, *2*, 207.

(18) Pong, W.; Smith, J. A. *J. Appl. Phys.* **1973**, *44*, 174.

(19) Kawai, T.; Soma, M.; Matsumoto, Y.; Onishi, T.; Tamaru, K. *Chem. Phys. Lett.* **1976**, *37*, 378.

(20) Kearns, D. R.; Calvin, M. *J. Chem. Phys.* **1961**, *34*, 2026.

(21) Pope, M. *J. Chem. Phys.* **1962**, *36*, 2810.

0002-7863/92/1514-8669$03.00/0 © 1992 American Chemical Society

These authors used photoelectric threshold measurements[20] and a technique similar to that employed by Millikan to obtain the charge of the electron.[21]

The works of Höchst et al.[22] and Battye et al.[23] constitute the first detailed photoemission studies on phthalocyanines. Höchst et al.[22] reported the XPS ($h\nu$ = 1487 eV) spectra of the valence bands of the β-polymorphic form of H_2Pc, FePc, CoPc, NiPC, CuPc, and the α-polymorphic form of PtPc and devoted special emphasis to the investigation of d-electron states of the central metal atom. These authors pointed out that the spectra of phthalocyanine appear to be a superposition of those of its molecular constituents pyrrole and benzene. Battye et al.[23] performed an UPS (He I and He II ($h\nu$ = 40.8 eV)) investigation of the outer valence bands of thin films of H_2Pc, FePc, CuPc, and PtPc down to above 18 eV below the Fermi level and remarked upon the similarity of the spectra. These authors were the first in trying to correlate the positions of structural features in the UPS spectra with theoretically calculated binding energies but found no satisfying correspondence.

Between 1977 and 1981, Koch and co-workers published a very complete collection of papers studying the electronic valence band of phthalocyanines.[24-30] In the first of these papers,[24] Koch and Grobman reported and discussed the Ne I ($h\nu$ = 16.8 eV), He I, and He II UPS spectra of thin polycrystalline films of MgPc and PbPc and compared them to the spectra of H_2Pc. They evidenced the close similarity between the phthalocyanine bands from 8.0 to ≈14 eV and the benzene spectrum and assigned the uppermost band at around 5.4-eV binding energy to a carbon π-molecular orbital on the basis of Pariser–Parr–Pople (PPP) semiempirical molecular orbital (MO) calculations.[31] In the following papers,[25-29] they studied particular aspects of various MPc's (PbPc, PtPc, NiPc, ZnPc, CuPc) using monochromatized synchrotron radiation up to 260 eV.

Especially interesting is the paper by Tegeler et al.[30] who measured and compared the soft X-ray emission and photoelectron emission spectra of H_2Pc, MgPc, and PtPc obtained with synchrotron radiation ($h\nu$ = 100 eV). They combined these techniques to resolve the electronic structure of the phthalocyanine valence band into the atomic constituents from a pure experimental approach. The assignment they performed shows serious limitations in recognizing nitrogen contributions and in disentangling σ and π characters. All the papers commented upon in this paragraph are in some way reviewed in ref 32.

To our knowledge and apart from the works by Koch et al. mentioned above, very scarce investigations have been performed on the photoemission valence band of phthalocyanines during the eighties. In 1983, Xian et al.[33] measured the threshold ionization potentials of α- and β-CuPc by means of UPS. This constitutes the first UPS study of polymorphs of a organic crystal with known structures. In 1987, Klofta et al.[34] recorded the He I UPS spectra of chlorogallium phthalocyanine (ClGaPc) thin films. Guay et al.[35] have recently reported a very detailed UPS (He I) and synchrotron radiation (120 eV) study to characterize the electronic structure of the similar ClAlPc and BrAlPc phthalocyanine thin films subjected to chemical transformations. In 1989, Göpel et al.[36,37] published XPS and UPS studies of the valence band structure of PbPc in the context of the film/substrate interfaces implied in hybrid molecular electronic devices such as organic/inorganic gas sensors.

The very recent works of Hino et al.[38] and Ozaki and Harada[39,40] merit special attention. Hino et al.[38] present the XPS and UPS (He I and He II) spectra of PtPc and its highly conducting radical salts $PtPc(ClO_4)_{0.5}$ and $PtPc(AsF_6)_{0.5}$. To our knowledge, this is the first photoemission study on partially oxidized phthalocyanines. The authors try to answer different questions concerning the electronic structure before and after the oxidation, which are directly related to the evolution of the electrical behavior in going from neutral to partially oxidized PtPc's. They find that UPS spectra of the radical salts and the neutral molecules are essentially the same, except for the absolute binding energies.

Ozaki and Harada[39,40] have measured the Penning ionization electron spectra (PIES) and He I UPS spectra for two kinds of ultrathin films of FePc showing different orientations of the molecules on the surface. In PIES, the electrons are ejected from the surface molecules by collision of these molecules with a beam of metastable rare gas atoms. The excitation energy of the metastable atom (e.g., He*-2^3S, 19.82 eV) is used to ionize the molecule, and the PIES spectrum is obtained by analyzing the kinetic energy distribution of the ejected electrons. One of the advantages of PIES relative to XPS or UPS techniques is that the intensity of PIES bands depends on the orientation of the surface molecules since only those MO's extending outside the repulsive part of the van der Waals surface are accessible to the beam of metastable atoms. This feature of PIES is exploited to reveal the character (σ, π, or 3d-like) of MO's responsible for PIES bands.

Finally, Fahy et al.[41] have recorded the photoelectron spectra of highly oriented films of the radical phthalocyanine dimer, $LuPc_2$, and the fluorine-bridged stacked phthalocyanine polymer $(FAlPc)_n$ using angle-resolved UPS and monochromatized synchrotron radiation. The spectra for both $LuPc_2$ and $(FAlPc)_n$ are found to be very similar to measurements on most other simple phthalocyanine compounds.

Besides all the solid-state investigations mentioned above,[16-19,22-30,32-41] phthalocyanine molecules have been the subject of a few photoemission studies in the gas phase. The most relevant of these studies corresponds to that reported by Berkowitz,[42] who performed a systematic study of the He I UPS spectra of H_2Pc and several MPc molecules. Hush and Cheung[43] and Ciliberto et al.[44] obtained the He I UPS spectra of a silicon phthalocyanine monomer and studied the splitting observed for the uppermost band in the dimer. Finally, Klofta et al.[34] also recorded the gas-phase He I UPS spectrum of ClGaPc.

The photoelectron energy distribution measurements on Pc's reveal a complex structure for the valence bands, extending over a binding energy range from 5 to 35 eV. This complex electronic structure has not been fully understood owing to the large number of molecular orbitals contributing to the density of states (in H_2Pc, there are 186 valence electrons occupying 93 MO's). In this paper,

---

(22) Höchst, H.; Goldmann, A.; Hüfner, S.; Malter, H. *Phys. Stat. Sol. B* **1976**, *76*, 559 (1976).

(23) Battye, F. L.; Goldmann, A.; Kasper, L. *Phys. Stat. Sol. B* **1977**, *80*, 425.

(24) Koch, E.-E.; Grobman, W. D. *J. Chem. Phys.* **1977**, *67*, 837.

(25) Iwan, M.; Eberhardt, W.; Kalkoffen, G.; Koch, E.-E.; Kunz, C. *Chem. Phys. Lett.* **1979**, *62*, 344.

(26) Iwan, M.; Koch, E.-E. *Solid State Commun.* **1979**, *31*, 261.

(27) Iwan, M.; Koch, E.-E.; Chiang, T. C.; Himpsel, F.-J. *Phys. Lett. A* **1980**, *76*, 177.

(28) Iwan, M.; Koch, E.-E.; Chiang, T. C.; Eastman, E. E.; Himpsel, F.-J. *Solid State Commun.* **1980**, *34*, 57.

(29) Koch, E.-E.; Iwan, M.; Hermann, K.; Bagus, P. S. *Chem. Phys.* **1981**, *59*, 249.

(30) Tegeler, E.; Iwan, M.; Koch, E.-E. *J. Electron Spectrosc. Rel. Phenom.* **1981**, *22*, 297.

(31) Henriksson, A.; Sandbom, M. *Theor. Chim. Acta* **1972**, *27*, 213.

(32) Koch, E.-E. In *Organic Molecular Aggregates*; Reinecker, P., Haken, H., Wolf, H. C., Eds.; Springer: Berlin, 1983; p 35.

(33) Xian, C. S.; Seki, K.; Inokuchi, H.; Zurong, S.; Renyuan, Q. *Bull. Chem. Soc. Jpn.* **1983**, *56*, 2565.

(34) Klofta, T. J.; Sims, T. D.; Pankow, J. W.; Danziger, J.; Nebesny, K. W.; Armstrong, N. R. *J. Phys. Chem.* **1987**, *91*, 5651.

(35) Guay, D.; Tourillon, G.; Gastonguay, L.; Dodelet, J. P.; Nebesny, K. W.; Armstrong, N. R.; Garrett, R. *J. Phys. Chem.* **1991**, *95*, 251.

(36) Mockert, H.; Schmeisser, D.; Göpel, W. *Sensors Actuators* **1989**, *19*, 159.

(37) Rager, A.; Gompf, B.; Dürselen, L.; Mockert, H.; Schmeisser, D.; Göpel, W. *J. Mol. Electron.* **1989**, *5*, 227.

(38) Hino, S.; Matsumoto, K.; Yamakado, H.; Yakushi, K.; Kuroda, H. *Synth. Met.* **1989**, *32*, 301.

(39) Ozaki, H.; Harada, Y. *J. Chem. Phys.* **1990**, *92*, 3184.

(40) Ozaki, H.; Harada, Y. *J. Am. Chem. Soc.* **1987**, *109*, 949.

(41) Fahy, M. R.; Fujimoto, H.; Dann, A. J.; Hoshi, H.; Inokuchi, H.; Manujama, Y.; Willis, M. R. *Phys. Scrip.* **1990**, *41*, 550.

(42) Berkowitz, J. *J. Chem. Phys.* **1979**, *70*, 2819.

(43) Hush, N. S.; Cheung, A. S. *Chem. Phys. Lett.* **1977**, *47*, 1.

(44) Ciliberto, E.; Doris, K. A.; Pietro, W. J.; Reisner, G. M.; Ellis, D. E.; Fragalā, I.; Herbstein, F. H.; Ratner, M. A.; Marks, T. J. *J. Am. Chem. Soc.* **1984**, *106*, 7748.

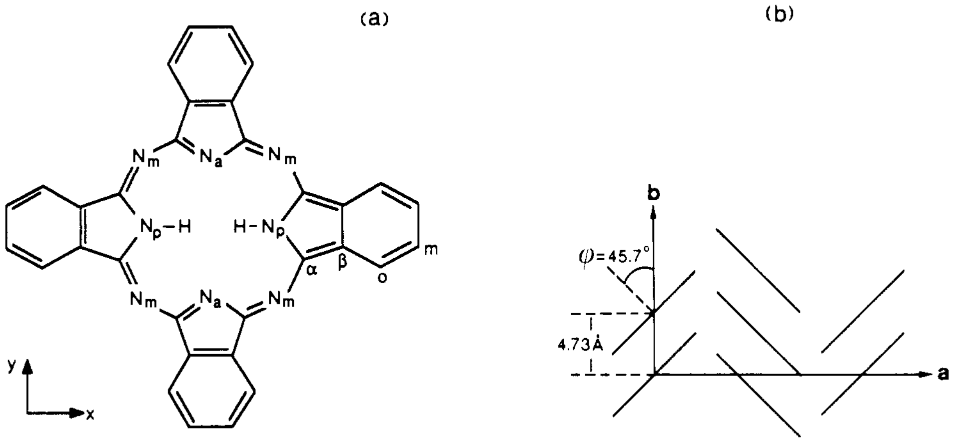

Figure 1. (a) Molecular structure of metal-free phthalocyanine. N_p denotes a pyrrole nitrogen and N_a and N_m indicate pyrrole aza and meso-bridging aza nitrogens, respectively. The carbon atoms are denoted following their position with respect to pyrrole nitrogen atoms (C_α and C_β) and to the pyrrole moiety (C_o and C_m). (b) Schematic drawing of the molecular packing of β-H_2Pc viewed along the *c* axis.

we perform a comprehensive theoretical analysis of the whole valence electronic band of phthalocyanines on the basis of nonempirical band structure calculations on phthalocyanine stacks and previous molecular calculations[45] on H_2Pc. Our main goal is to provide a theoretical basis that allows for the full interpretation of the photoemission solid-state data detailed above. We have chosen H_2Pc (see Figure 1a) as a reference system because valence band photoemission features appear to be, as discussed before, rather insensitive to the presence of metal atoms, and they are largely determined by the conjugated macrocycle structure.[23,24,41] This fact is explained as a consequence of the low proportion of metal to Pc electrons and of the small cross sections of metal d-electrons at low photon energies. To the best of our knowledge, only one theoretical attempt of simulating the photoelectron spectra of phthalocyanines has been reported using local-density-functional (LDF) electronic structure calculations.[46] Phthalocyanine compounds have been the object of a very large number of molecular[31,47–51] and band structure calculations.[51b,52–55] However, most of these calculations have been performed at a semiempirical level and using simplified molecular models because of the large size and complexity of the phthalocyanine system, $C_{32}N_8H_{18}$. In this work, we make use of the nonempirical valence effective Hamiltonian (VEH) pseudopotential method. The validity of the VEH approach to study the electronic structure of phthalocyanines has been widely illustrated in previous works.[45,56,57]

II. Computational Aspects

All the calculations reported here have been performed in the framework of the VEH quantum-chemical technique which was originally developed for molecules[58] and later extended to deal with stereoregular infinite chain systems.[59] The VEH method takes into account the valence electrons and is parameterized to reproduce the results of ab initio double-zeta (ζ) Hartree–Fock calculations without performing any self-consistent-field (SCF) process or calculating any bielectronic integral. These features convert the VEH method in an especially useful tool to deal with very large molecular or crystalline systems since it yields one-electron energies of ab initio double-ζ quality at a reasonable computer cost. VEH band structure calculations have been carried out using the atomic potentials previously optimized for hydrogen, carbon, and nitrogen.[60,61]

The density of valence states (DOVS) has been calculated from the band structure following the methodology of Delhalle and Delhalle.[62] In order to compare the theoretically computed DOVS curves to the experimental photoemission spectra, a three-step procedure has to be used and consists of (i) the convolution of the bare DOVS curves by a Gaussian function of adjustable full width at half-maximum (fwhm), (this is a way of introducing in our theoretical simulation the static and dynamic disorder effects that exist in the solid state and cause the broadening of the photoemission line widths with respect to the gas phase); (ii) the application of a rigid shift of the DOVS curves toward lower binding energies in order to deal with the solid-state polarization energy due to interchain relaxation effects; and (iii) the contraction of the VEH DOVS curves along the energy scale in order to correct for the too wide valence band that Hartree–Fock ab initio calculations and, therefore, VEH calculations provide. This procedure has been successfully used previously for a variety of polymeric systems.[63–65]

---

(45) Ortí, E.; Brédas, J. L. *J. Chem. Phys.* **1988**, *89*, 1009.

(46) Mintmire, J. W.; Kutzler, F. W.; White, C. T. *Phys. Rev. B* **1987**, *36*, 3312.

(47) Pullman, A.; Berthier, G. *C. R. Acad. Sci. Paris* **1953**, *236*, 1494. Basu, S. *Ind. J. Phys.* **1954**, *28*, 511. Gouterman, M.; Wagniere, G. H.; Snyder, L. L. *J. Mol. Spectrosc.* **1963**, *11*, 103. Chen, I. *Ibid.* **1967**, *23*, 131. Chen, I.; Abkowitz, M. *J. Chem. Phys.* **1969**, *50*, 2237.

(48) Schaffer, A. M.; Gouterman, M. *Theor. Chim. Acta* **1972**, *25*, 62. Edwards, L.; Gouterman, M. *J. Mol. Spectrosc.* **1970**, *33*, 292. Schaffer, A. M.; Gouterman, M.; Davidson, E. R. *Theor. Chim. Acta* **1973**, *30*, 9.

(49) Weiss, C.; Kobayashi, H.; Gouterman, M. *J. Mol. Spectrosc.* **1965**, *16*, 415; **1970**, *33*, 292. Henriksson, A.; Roos, B.; Sundbom, M. *Ibid.* **1972**, *27*, 303. McHugh, A. J.; Gouterman, M.; Weiss, C., Jr. *Ibid.* **1972**, *24*, 346.

(50) Lee, L. K.; Sabelli, N. H.; LeBreton, P. R. *J. Phys. Chem.* **1982**, *86*, 3926.

(51) (a) Berkovitch-Yellin, Z.; Ellis, D. E. *J. Am. Chem. Soc.* **1981**, *103*, 6066. (b) Kutzler, F. W.; Ellis, D. E. *J. Chem. Phys.* **1986**, *84*, 1033.

(52) Chen, I. *J. Chem. Phys.* **1969**, *51*, 3241. Sukigara, M.; Nelson, R. C. *Mol. Phys.* **1969**, *17*, 387. Mathur, S.; Singh, J.; Singh, D. C. *J. Phys. C* **1971**, *4*, 3122. Honeybourne, C. L. *Mol. Phys.* **1983**, *50*, 1045.

(53) Böhm, M. C. *Phys. Rev. B* **1983**, *28*, 6914. *Chem. Phys.* **1984**, *86*, 17. Böhm, M. C.; Ramírez, R.; Oles, A. M. *Ibid.* **1987**, *117*, 405. Ramírez, R.; Böhm, M. C. *Int. J. Quantum Chem.* **1988**, *33*, 73.

(54) Whangbo, M.-H.; Stewart, K. R. *Isr. J. Chem.* **1983**, *23*, 133. Canadell, E.; Alvarez, S. *Inorg. Chem.* **1984**, *23*, 573. Gómez-Romero, P.; Lee, Y.-S.; Kertesz, M. *Ibid.* **1988**, *27*, 3672.

(55) Pietro, W. J.; Marks, T. J.; Ratner, M. A. *J. Am. Chem. Soc.* **1985**, *107*, 5387. Hale, P. D.; Ratner, M. A. *J. Chem. Phys.* **1985**, *83*, 5277.

(56) Ortí, E.; Brédas, J. L.; Clarisse, C. *J. Chem. Phys.* **1990**, *92*, 1228.

(57) Ortí, E.; Piqueras, M. C.; Crespo, R.; Brédas, J. L. *Chem. Mater.* **1990**, *2*, 110.

(58) Nicolas, G.; Durand, Ph. *J. Chem. Phys.* **1979**, *70*, 2020; **1980**, *72*, 453.

(59) André, J. M.; Burke, L. A.; Delhalle, J.; Nicolas, G.; Durand, Ph. *Int. J. Quantum Chem. Symp.* **1979**, *13*, 283.

(60) Brédas, J. L.; Chance, R. R.; Silbey, R.; Nicolas, G.; Durand, Ph. *J. Chem. Phys.* **1981**, *75*, 255.

(61) Brédas, J. L.; Thémans, B.; André, J. M. *J. Chem. Phys.* **1983**, *78*, 6137. Brédas, J. L.; Silbey, R.; Boudreaux, D. S.; Chance, R. R. *J. Am. Chem. Soc.* **1983**, *105*, 6555.

(62) Delhalle, J.; Delhalle, S. *Int. J. Quantum Chem.* **1977**, *11*, 349.

(63) Brédas, J. L.; Salaneck, W. R. *J. Chem. Phys.* **1986**, *85*, 2219. Lazzaroni, R.; Riga, J.; Verbist, J.; Brédas, J. L.; Wudl, F. *Ibid.* **1988**, *88*, 4257.

(64) Kowlaczyk, S. P.; Stafström, S.; Brédas, J. L.; Salaneck, W. R.; Jordan-Sweet, J. L. *Phys. Rev. B* **1990**, *41*, 1645. Lazzaroni, R.; Sato, N.; Salaneck, W. R.; Dos Santos, M. C.; Brédas, J. L.; Tooze, B.; Clark, D. T. *Chem. Phys. Lett.* **1990**, *175*, 175.

(65) (a) Ortí, E.; Stafström, S.; Brédas, J. L. *Chem. Phys. Lett.* **1989**, *164*, 240. (b) Ortí, E.; Brédas, J. L.; Pireaux, J. J.; Ishihara, N. *J. Electron Spectrosc. Rel. Phenom.* **1990**, *52*, 551.

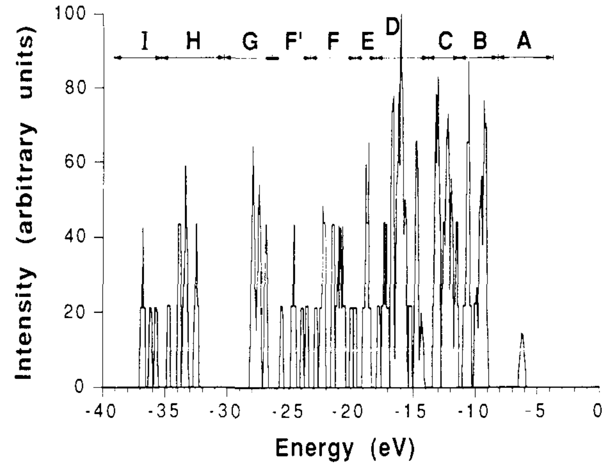

Figure 2. VEH calculated density of occupied valence states for β-H_2Pc.

To obtain a theoretical simulation of the XPS spectra, it is necessary to take into account an additional factor in order to include the effect of relative photoionization intensities of the crystal orbitals in the DOVS curves. To do so, we have used the Gelius model,[66] as extended to polymers.[67] This model relates the photoionization intensity, I_n, of the nth one-electron level to (i) the Mulliken gross atomic population and (ii) the experimental relative photoionization cross sections, σ_p, of the atomic orbital χ_p used in the LCAO (linear combination of atomic orbitals) expansion:

$$I_n(k) \propto \sum_p C_{np}(k)[\sum_q S_{pq}(k)C_{nq}(k)]\sigma_p$$

In this expression, C_{np} and C_{nq} denote the coefficients of the LCAO expansion and S_{pq} is the overlap integral between χ_p and χ_q. The p and q summations run over the set of atomic orbitals. The values used for σ_p are the following:[66] $\sigma(\mathrm{N, 2s}) = 1.2$, $\sigma(\mathrm{N, 2p}) = 1.2/11$, $\sigma(\mathrm{C, 2s}) = 1$, $\sigma(\mathrm{C, 2p}) = 1/13$, $\sigma(\mathrm{H, 1s}) = 0$; $\sigma(\mathrm{C, 2s}) = 1$, being taken as a reference.

Phthalocyanines crystallize in columnar stacks where the planar macrocyclic molecules lie parallel to one another as depicted in Figure 1b. This molecular packing determines a direct π–π interaction between adjacent molecules in the stack but very weak interactions between molecules in adjacent stacks. In this way, one-dimensional VEH band structure calculations have been performed along the direction which gives rise to a significant π-interaction, i.e., the stacking direction. Calculations have been carried out for both the α- and β-polymorphic forms of H_2Pc. These forms are the most common polymorphs of Pc's and mainly differ from one another in the degree of slipping in the columnar stacks, i.e., in the angle φ formed by the stacking axis and the normal to the molecular plane (see Figure 1b). φ takes values of about 25° for the α-polymorphs but increases to about 45° for the β-polymorphs. The crystalline structures used for α- and β-H_2Pc are those reported by Ashida et al. (b = 3.814 Å, φ = 26.5°)[68] and Hoskins et al. (b = 4.73 Å, φ = 45.7°).[69] The geometrical parameters used for the H_2Pc macrocycle are in both cases the same and correspond to the D_{2h} molecular geometry detailed in ref 57. As explained there, this geometry is based on the neutron diffraction data reported by Hoskins et al.[69] Since, as will be shown below, both polymorphic forms lead to almost identical results, only the results obtained for the β-form will be discussed in detail.

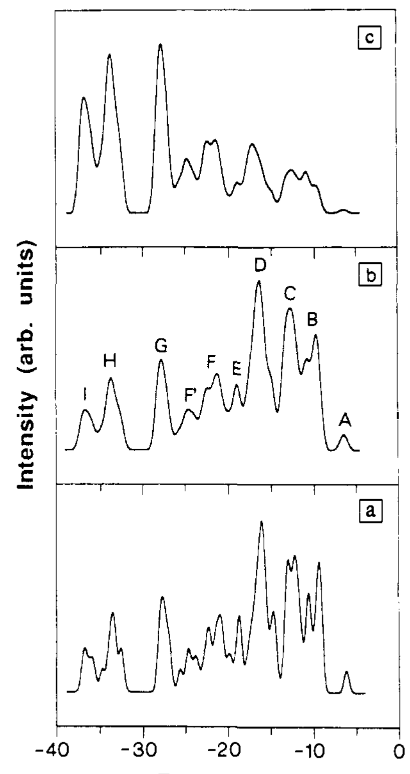

Figure 3. Convoluted VEH–DOVS curves for (a) the H_2Pc molecule (UPS simulation), (b) β-H_2Pc (UPS simulation), and (c) β-H_2Pc (XPS simulation). Convolution of the electronic states are performed by Gaussians with fwhf of 0.7 eV (a) and 1.0 eV (b and c). Labels correspond to those displayed in Figure 2.

Finally, we note that in going from H_2Pc to metallophthalocyanine, the symmetry of the macrocycle evolves from D_{2h} to D_{4h}; this might affect somewhat the appearance and energies of some of the energetically deeper bands (caution should thus be exerted when comparing our simulated valence band spectra for H_2Pc to those of metallophthalocyanines).

III. Results and Discussion

A. Theoretical Spectra. The VEH electronic density of valence states (DOVS) obtained for the β-polymorphic form of metal-free phthalocyanine is presented in Figure 2. It has been computed from the one-dimensional band structure calculated for β-H_2Pc along the stacking axis b (see Figure 1b). This band structure looks rather complicated since it is constituted, on the one hand, by a set of as many as 92 valence bands spanning an energy range of only 27.9 eV (−36.90 to −8.99 eV) and, on the other hand, by the HOCO (highest occupied crystalline orbital) band, which stands alone well above (−6.32 to −5.99 eV) the previous group of bands. All the valence bands show very small widths, the larger dispersions (0.32 to 0.40 eV) being found for bands of π-nature like the HOCO band (0.33 eV). This feature indicates that electron delocalization along phthalocyanine stacks is not very effective and that the electronic states in β-H_2Pc are mostly localized within single phthalocyanine molecules. This result is in accord with the fact that the interactions between adjacent molecules along the crystal stacks are essentially of van der Waals type.

Before comparing the theoretical results to the experimental photoelectron spectra, it is useful to analyze the nature of the different peak structures seen in the DOVS curves in order to be in a position to assign accurately the photoemission features. This analysis is usually undertaken on the basis of the atomic contributions to the electronic bands; it is more difficult in the case of β-H_2Pc owing to the large number of bands involved in each structure (e.g., 22 bands contribute to peak structure D in Figure

---

[66] Gelius, U. In *Electron Spectroscopy*; Shirley, D. A., Ed.; North-Holland: Amsterdam, 1972; p 311.

[67] Delhalle, J.; Delhalle, S.; André, J. M. *Chem. Phys. Lett* **1975**, *34*, 430.

[68] Ashida, M.; Uyeda, N.; Suito, E. *Bull. Chem. Soc. Jpn.* **1966**, *39*, 2616. Debe, M. K. *J. Appl. Phys.* **1984**, *55*, 3354.

[69] Hoskins, B. F.; Mason, S. A.; White, J. C. B. *J. Chem. Soc., Chem. Commun.* **1969**, 554.

[70] Brédas, J. L.; Chance, R. R.; Baughman, R. H.; Silbey, R. *J. Chem. Phys.* **1982**, *76*, 3673. Brédas, J. L.; Chance, R. R.; Silbey, R.; Nicolas, G.; Durand, Ph. *Ibid.* **1982**, *77*, 371. Brédas, J. L.; Elsembaumer, R. L.; Chance, R. R.; Silbey, R. *Ibid.* **1983**, *78*, 5656.

Table I. VEH Energies (in eV) Corresponding to the Most Salient Features of the Valence Electronic Density of States Spectra Displayed in Figure 3 for the H_2Pc Molecule (UPS Simulation) and the β-H_2Pc Crystal Polymorph (UPS or XPS Simulations)[a]

feature	molecule (UPS)[b]	β-H_2Pc (UPS)[b]	β-H_2Pc (UPS)[c]	α-H_2Pc (UPS)[c]	β-H_2Pc (XPS)[c]
I	−36.72	−36.77	−36.59	−36.56	−36.61
	−35.98	−36.06			
H	−34.64	−34.64			
	−33.47	−33.53	−33.53	−33.53	−33.53
	−32.49	−32.56			
G	−27.67	−27.71	−27.63	−27.62	−27.60
F′	−25.55	−25.68			
	−24.58	−24.63	−24.48	−24.48	−24.58
	−23.77	−23.83			
F	−22.24	−22.30	−22.17	−22.18	−22.19
	−20.92	−20.99	−21.08	−21.08	−21.25
	−19.78	−19.84			
E	−18.67	−18.73	−18.73	−18.73	−18.65
D	−15.92	−16.05	−16.14	−16.16	−16.90
	−14.70	−14.74			
C	−13.08	−12.99	−12.49	−12.39	−12.34
	−12.20	−12.28			
B	−10.60	−10.63	−10.54	−10.54	−10.68
	−9.22	−9.40	−9.48	−9.48	−9.55
A	−6.15	−6.21	−6.21	−6.20	−6.21

[a] The VEH results obtained for α-H_2Pc are also included for the sake of comparison. See Figure 3 for labels. [b] Convolution is performed by Gaussians with fwhm = 0.7 eV (*b*) or 1.0 eV (*c*).

2). To facilitate our analysis, we have taken into account the fact that, as discussed above, the electronic structure of the phthalocyanine molecule remains almost unaffected in the crystal. This is evidenced in Figure 3 and Table I, where the convoluted DOVS previously calculated for the phthalocyanine molecule (Figure 3a)[45] is compared with those obtained for β-H_2Pc (Figure 3, b and c).

The convoluted DOVS curves displayed in Figure 3, b and c, constitute a theoretical simulation of the photoemission UPS and XPS spectra of β-H_2Pc, respectively. They have been obtained following the methodology discussed in section II using a fwhm of 1.0 eV for the Gaussian functions. This factor is larger than the 0.7 eV value used in the molecular case (Figure 3a) in order to take into account the broadening that photoemission bands experience in the solid state. The peak structures appearing in Figure 3 are identified by labels A to J, which correspond to those displayed in Figure 2 and to those previously used in the experimental photoemission spectra of Tegeler et al.[30] These labels are employed in Table I (where the energies of the different peaks are listed) and in the following discussion.

A one-to-one correspondence can be established from Figure 3 between the peak structures of the H_2Pc molecule and those of the β-H_2Pc crystal. This correspondence is clearly observed in Table I, where the energies computed for the UPS peaks of β-H_2Pc using a convolution factor of 0.7 eV (instead of 1.0 eV) are also included. As can be seen, all the peaks reported for the molecule appear at almost the same energies for the crystal. Table I also collects the VEH results obtained for the α-polymorphic form of H_2Pc. The UPS peak energies calculated for this form are mostly identical with those of β-H_2Pc. The result confirms again that the electronic structure of the crystal mainly corresponds to that of the single phthalocyanine molecules and indicates that minor changes are to be expected upon modification of the crystalline structure.

The atomic origin of the DOVS peak structures in β-H_2Pc can thus undoubtedly be identified with that of the corresponding peak structures in the molecule. The analysis of the valence band of the H_2Pc molecule has been previously performed[45] and leads to the following assignments. Structure I in Figure 3 comes from the 2s atomic orbitals of the N_p, N_a, and C_α atoms (see Figure 1a for atomic labels). The main peak of structure H results from 2s contributions of all the carbon atoms forming the benzene moieties in H_2Pc and clearly corresponds to the totally bonding $1a_{1g}$ molecular orbital of benzene (see Table I in ref 65b for a detailed picture of the benzene molecular levels). Shoulders at higher and lower energies originate in nitrogen 2s orbitals. Peak G involves 2s contributions from C_o or C_β and C_m orbitals, much as in the degenerate $1e_{1u}$ molecular orbitals of benzene. Small peak F′ mostly originates in C_α 2s orbitals. The two peaks constituting structure F are associated with benzene moieties. The peak at higher binding energies has the same atomic composition as the degenerate C_{2s} $1e_{2g}$ orbitals of benzene, and that at lower binding energies corresponds to the C_{2p}–H_{1s} bonding as in the benzene $2a_{1g}$ orbital. Peak E mainly results from 2p σ-electronic levels from the nitrogen and carbon atoms forming the central ring skeleton of phthalocyanine macrocycle.

As mentioned above, 22 different electronic levels are involved in peak D, the most intense in the theoretical UPS simulation. On the high-energy side, a group of four levels centered around 17.0 eV and composed of 2s (carbon) and 1s (hydrogen) contributions of benzene is found. These levels clearly correlate with the strongly bonding C_{2s}–H_{1s} $1b_{1u}$ molecular orbital of benzene which is calculated at almost the same energy (17.05 eV).[65b] The relevance of these levels is discussed below. The main group of levels contributing to peak D show the same composition as the C_{2p}–C_{2p} $1b_{2u}$ and C_{2p}–H_{1s} $2e_{1u}$ σ-bonding orbitals of benzene.

Structure C centered at −12.49 eV mainly results from the totally bonding $1a_{2u}$ π molecular orbital of benzene at higher binding energies ($\approx$13.0 eV) and from N_a electron lone pairs and nitrogen $2p_z$ orbitals at lower binding energies ($\approx$12.2 eV). Important contributions from C_{2p}–C_{2p} and C_{2p}–H_{1s} $2e_{2g}$ benzene orbitals are also observed. The origin of the peaks forming structure B is clearly defined. The low-energy peak corresponds to the σ electron lone pairs of N_m atoms. The high energy peak is of π nature and originates in the highest occupied $1e_{1g}$ orbitals of benzene with some contributions from N_p and N_a atoms. Finally, small peak A can be clearly assigned since it comes exclusively from the HOCO band. This band originates in the overlap of the $4a_u$ π orbitals (in D_{2h} symmetry) fo phthalocyanine molecules; it does not show any contribution from nitrogen atoms as sketched in ref 45.

As can be seen from Figure 3 and Table I, the theoretical XPS simulation of β-H_2Pc shows the same overall features as the UPS simulation. The main difference between these spectra is the dramatic decrease of intensity that the XPS spectrum experiences on the low binding energy region due to the small cross-section factors of 2p atomic orbitals relative to 2s atomic orbitals. Consequently, the most intense XPS structure corresponds to the C_{2s} peak G instead of the C_{2p} peak D (see Figure 3, b and c, respectively). The positions and assignments of the peaks are the same as for the UPS spectrum, and only peak D shows a noticeable shift from −16.14 eV (UPS) to −16.90 eV (XPS). This evolution originates in the presence of strong contributions from C_{2s} $1b_{1u}$ orbitals of the benzene moieties on the high-binding energy side of the peak, as detailed above. Note the almost complete disappearance of the lowest binding energy peak A in the XPS spectrum as a result of its C_{2p} π nature.

B. Correlation with Experimental Photoemission Spectra. From the preceding analysis, it is clear that the electronic structure of the benzene moieties is preserved in metal-free phthalocyanine, and a direct correlation between most of the peak structures calculated for H_2Pc and the one-electron energy levels of benzene can be established. This correspondence was first suggested by Höchst et al.,[22] who predicted that the photoelectron spectra of phthalocyanines appear to be a superposition of their molecular constituents pyrrole and benzene. This prediction is not confirmed for pyrrole since almost no molecular orbitals pertaining to pyrrole can be identified in the electronic structure of phthalocyanine and it is the central macrocycle backbone which mostly accounts for the electronic contributions of N_p, N_a, and C_α atoms. We thus conclude that, from an electronic structure standpoint, phthalocyanine can be visualized as the result of joining four benzene rings to the central carbon–nitrogen ring.

In Figure 4, we compare the VEH–DOVS spectra (UPS and XPS simulations) calculated for β-H_2Pc with the solid-state synchrotron ($h\nu$ = 100 eV) and XPS ($h\nu$ = 1487 eV) photoemission spectra reported by Tegeler et al.[30] and Höchst et al.,[22]

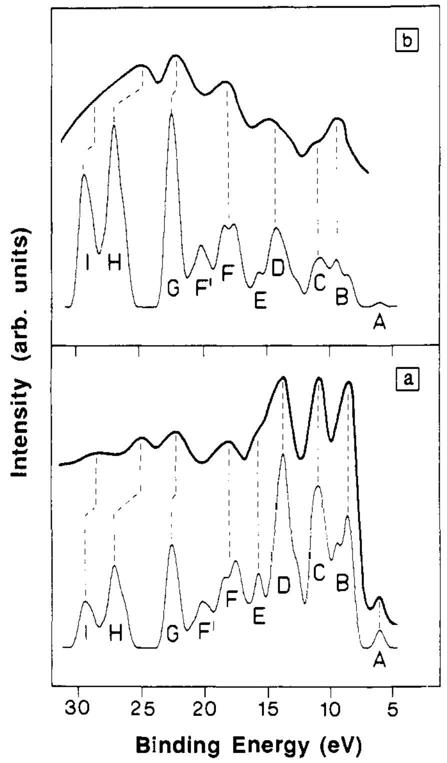

Figure 4. Theoretical VEH and experimental solid-state photoemission valence band spectra of metal-free phthalocyanine: (a) theoretical UPS simulation (lower curve) together with synchrotron data[30] (upper curve); (b) theoretical XPS simulation (lower curve) together with XPS spectrum[22] (upper curve). Theoretical spectra are contracted and shifted as discussed in the text. Labels correspond to those displayed in Figures 2 and 3.

Table II. Calculated (VEH-UPS and -XPS) and Measured Binding Energies (eV) for the Most Salient Features of the Valence Band of β-H_2Pc[a]

	feature[b]	VEH-UPS[c]	ref 30[d]	ref 35[a]	VEH-XPS[a]
I	(N_p, N_a - 2s)	29.27	28.2		29.28
H	(C_{2s}, $1a_{1g}$)	26.92	24.9	24.9	26.92
G	(C_{2s}, $1e_{1u}$)	22.38	21.9	21.8	22.35
F′	(C_α-2s)	19.95			20.03
F	(C_{2s}, $1e_{2g}$)	18.18	18.0	18.0	18.19
	(C_{2p}-H_{1s}, $2a_{1g}$)	17.34			17.47
E	(C_{2p}, N_{2p} central ring)	15.53	15.4	15.2	15.47
D	(C_{2s}-H_{1s}, $1b_{1u}$)				14.12
	(C_{2p}-H_{1s}, $1b_{2u}$ + $2e_{1u}$)	13.54	13.6	13.5	
C	(C_{2p}, $1a_{2u}$ + $2e_{2g}$, + N_a electron lone pairs)	10.73	11.0	11.1	10.62
B	(N_m electron lone pairs)	9.23			9.34
	(C_{2p}, $1e_{1g}$ π)	8.42	8.6	8.5	8.47
A	(C_{2p}, $4a_u$ π-MO)	5.90	5.9	5.9	5.90

[a] All the energies are referred to the vacuum level, E_{vac} = 0.0 eV. [b] Labels correspond to those displayed in Figures 2 to 4. The main atomic contributions are indicated in parentheses according to section III.A. Contributions from the benzene moieties are denoted by the symmetry labels of the corresponding MO's of benzene. $4a_u$ π-MO in feature A refers to H_2Pc in D_{2h} symmetry. [c] VEH binding energies calculated from Table I after a contraction of 1.3 of the energy scale and a rigid shift of the valence band to match the first experimental feature at 5.9 eV. [d] Photoemission energies measured for thin polycrystalline films of H_2Pc using an excitation energy of 100 eV. The estimated error due to inherent width of the photoemission bands and overall experimental resolution is ±0.2 eV. [e] Energies observed for ClAlPc thin films using excitation energies of 21.2 and 120.0 eV.

respectively. The theoretical spectra have been contracted by a factor of 1.3 eV, the same as that used in previous VEH studies,[45,63-65] and shifted by 0.31 eV to lower binding energies to match the first experimental synchrotron peak located at 5.9 eV. The resulting energies are collected in Table II together with the experimental binding energies reported for polycrystalline films of H_2Pc by Tegeler et al.[30] The photoemission energies obtained for the related compound ClAlPc are also included.[35] To compare with the theoretical UPS spectrum in Figure 4a, we prefer to make use of the experimental synchrotron ($h\nu$ = 100 eV) spectrum,[30] rather than other UPS (He I or He II) spectra reported in the literature,[23,24] because it presents better resolution and covers a wider range of binding energies.

As can be seen from Figure 4 and Table II, the relative peak positions and intensities predicted by the VEH theoretical simulations are found to be in excellent agreement with the UPS and XPS experimental data. A one-to-one correspondence can therefore be established between the theoretical peak structures and the experimental photoemission bands. Starting from higher binding energies, theoretical peak I calculated at 29.27 eV and mainly coming from N_p and N_a 2s orbitals can be correlated with the diffuse experimental feature observed about 28.2 eV. In the same way, the carbon 2s peak H located at 26.92 eV can be associated with the photoemission band centered at 24.9 eV. We note that the correlation between theory and experiment is weaker for the valence structures at higher binding energies. However, this is an expected result since the VEH method was mainly parameterized to reproduce the top of the valence band.[59,60,70] Indeed, the VEH method calculates the C_{2s} $1a_{1g}$ orbital of benzene, which mainly gives rise to peak H, to be 2.2 eV too high in binding energy.[45,65b] If we subtract this quantity from the VEH energy of peak H, the agreement between theory (24.72 eV) and experiment (24.9 eV) is again very good.

The synchrotron band at 21.9 eV corresponds to theoretical peak G which gives rise to the most intense structure in the XPS spectrum. This peak (originating in the C_{2s} $1e_{1u}$ molecular orbitals of benzene) is calculated 0.48 eV too high in energy as is also the case in the parent benzene molecule (0.34 eV).[45,65b] The next experimental feature is located at about 18.0 eV, just between the two theoretical peaks forming structure F (coming from C_{2s} $1e_{2g}$ and C_{2p} $2a_{1g}$ levels of benzene moieties). Since the carbon 2s levels contribute more strongly to the higher binding energy peak, this atomic composition explains the small shift to higher binding energies that the photoemission band experiences in going from UPS to XPS spectra. The fact that no experimental band is detected around 20 eV to correlate with theoretical structure F′ can be explained by the relative low intensity (especially in the XPS case) of this peak compared with adjacent structures (see Figure 4). Our assignment of the photoemission bands at 21.9 and 18.0 eV confirms that previously proposed by Tegeler et al.[30] on a pure experimental basis. On the one hand, these authors predict that both bands are mainly due to 2s contributions since the X-ray 2p → 1s emission spectra show very low intensities in this energy range for both the carbon and nitrogen emission and only some 2p → 1s carbon emission is detected for the band at 18.0 eV. On the other hand, they demonstrate that both bands are predominantly due to carbon 2s by comparing the XPS features of H_2Pc and solid benzene. All these observations are in perfect agreement with the atomic contributions we theoretically predict for band G (C_{2s}) and band F (C_{2s} and C_{2p}).

We now turn to a discussion of the outer part of the valence band, from 16 to 5 eV. The intense and broad synchrotron band measured at 13.6 eV perfectly corrlates with the highest theoretical peak D calculated at 13.54 eV. The experimental band shows a shoulder on its high binding energy side (15.4 eV) that corresponds to peak E (15.53 eV). This shoulder is not observed in the XPS spectrum because peak E comes only from carbon and nitrogen 2p orbitals which have very low cross sections. Furthermore, peak D experiences a shift to higher binding energies in going from UPS to XPS spectra due to the contributions of the C_{2s}-H_{1s} $1b_{1u}$ levels of benzene moieties at about 14.12 eV. This shift is clearly observed when comparing the experimental synchrotron and XPS spectra (see Figure 4). The atomic compositions predicted both for peak D and shoulder E are in perfect agreement with the experimental assignments reported by Tegeler et al.[30]

The experimental band observed at 11.0 eV is assigned to theoretical peak C calculated at 10.73 eV. As summarized in Table II, this peak involves contributions from C_{2p} $1a_{2u}$ (π) and $2e_{2g}$ (σ) orbitals of benzenes and N_a electron lone pairs, and it constitutes the first feature involving π contributions. The mixed π and σ character we predict for peak C corroborates the assignment performed by Ozaki et al.[39] by comparing the UPS and PIES spectra measured for two kinds of ultrathin films of FePc with different orientation of the surface molecules.

Much controversy exists in the literature about the assignment of the photoemission band at 8.6 eV. Kawai et al.[19] and Guay et al.[35] suggest that this band arises from the electron lone pairs of the meso-bridging aza nitrogens N_m on the basis of the PPP calculations of Henriksson et al. for CuPc.[49] Oppositely, Ozaki et al.[39] only identifies π-molecular orbital contributions to this band from their PIES experiments. Finally, Tegeler et al.[30] propose that both carbon and nitrogen 2p orbitals contribute to this band but are unable to disentangle further the σ or π character of the contributions.

Our VEH calculations help to assign properly the photoemission band at 8.6 eV, which is clearly associated with theoretical structure B (see Figure 4 and Table II). This structure consists of two peaks coming from N_m electron lone pairs (9.23 eV) and carbon $1e_{1g}$ π orbitals of benzene (8.42 eV), respectively. Therefore, both nitrogen lone pairs and carbon π orbitals are involved in the experimental feature B at 8.6 eV. The double peak structure of B, however, is actually an artifact of the theoretical calculations since the VEH method locates, as many other ab initio methods, the lone pairs of nitrogen atoms too high in binding energy. Molecular calculations on model compounds such as pyrazine, pyrimidine, and *s*-triazine show that the VEH method overestimates the binding energy of nitrogen lone pairs by about 0.7 eV compared to experimental gas-phase ionization potentials.[71] If we subtract 0.7 eV to 9.23 eV in structure B, we find an unique peak centered at 8.5 eV in perfect agreement with experiment. These facts explain why the peak at 9.23 eV has no correspondence in the higher-resolution gas-phase UPS spectrum reported by Berkowitz[42] for H_2Pc as it is shown in ref 45.

Finally, the lowest binding energy photoemission band at 5.9 eV unambiguously corresponds to the ionization of the C_{2p} $4a_u$ π-electronic level of phthalocyanine macrocycles (peak A) which, as mentioned before, shows no contribution from nitrogen atoms. This peak has been wrongly assigned in recent works to dynamic effects[46] and to the presence of various macrocyclic π orbitals[39] on the basis of ab initio calculations for the related porphine molecule.[72] However, we have shown[73] that the second HOMO of porphine is separated by only 0.5 eV from the $2a_u$ HOMO and by 1.9 eV from the rest of the occupied orbitals, in sharp contrast to the situation found for H_2Pc where the $4a_u$ HOMO lies alone 2.3 eV above the rest of the occupied orbitals.[45,56] Guay et al.[35] also suggest that peak A contains nitrogen lone pairs contributions since they observe a continuous decrease of this peak due to the protonation of N_m atoms. We think, however, that this protonation implies modifications in the electronic and geometrical structure of phthalocyanine which could explain the changes experienced by peak A, without having to invoke the presence of nitrogen contributions. Moreover, peak A is not observed in the XPS spectrum of Figure 4b owing to the low cross sections of C_{2p} orbitals at high-photon energies.

As mentioned in the Introduction, Xian et al.[33] predict a threshold ionization potential for the β-polymorphic form of phthalocyanine 0.2 eV lower than that observed for the α-polymorph. We can explain this result as a consequence of the different VEH bandwidths obtained for both polymorphs. The width of the HOMO band is calculated to have a value of 0.11 eV for α-H_2Pc and broadens to 0.33 eV for β-H_2Pc. This broadening determines that the threshold ionization energy theoretically predicted for β-H_2Pc (5.99 eV) is 0.14 eV lower than that calculated for α-H_2Pc (6.13 eV).

To end this discussion, we would like to mention the splitting that band A experiences for dimeric phthalocyanine compounds. This splitting was first observed for silicon phthalocyanine dimers in the gas phase[43,44] and has been recently reported for $LuPc_2$ dimers in the solid state.[41] The splitting can be explained in the light of VEH calculations on phthalocyanine dimers[56] which predict the doubling of the $4a_u$ HOMO level in passing from monomeric to dimeric phthalocyanines due to the interaction between both rings. The VEH results predict a splitting of 0.35 eV for silicon phthalocyanine dimers and of 0.83 eV for $LuPc_2$, in very good agreement with experimental data (0.29–0.32 eV[43,44] and 0.7 eV,[41] respectively). The larger splitting observed for $LuPc_2$ is due to the stronger interaction that takes place between the phthalocyanine rings in this compound, where the mean separation between the Pc planes is only 2.69 Å compared to an inter-ring distance of 3.32 Å in the silicon compound.

IV. Synopsis

We have investigated the electronic structure of one-dimensional stacks of metal-free phthalocyanine using the valence effective Hamiltonian (VEH) nonempirical technique. The small widths calculated for the electronic valence bands reveal that electronic states in β-H_2Pc are highly localized within single phthalocyanine molecules. Furthermore, the similarity of the DOVS curves obtained for β-H_2Pc and those previously reported for the isolated molecule[45] points out that the electronic structure of the latter remains almost unaffected in the crystal. On this basis and in order to achieve a detailed analysis of the electronic structure of β-H_2Pc, we have performed a one-to-one correspondence between the electronic peak structures that constitute the VEH–DOVS curves of the molecule and the crystal. This analysis shows that the electronic characteristics of the benzene moieties are preserved in the phthalocyanine macrocycle and that phthalocyanine must be viewed as the result of joining four benzene rings to the central carbon–nitrogen methineimine-like ring.

The VEH–DOVS curves convoluted to simulate UPS and XPS spectra have been compared with experimental solid-state synchrotron and XPS spectra. The theoretical curves are fully consistent with the solid-state spectra, and an excellent quantitative agreement between theory and experiment is found when comparing the positions of the main peaks. A complete interpretation of all the features appearing in the photoemission spectra is performed in the light of the VEH predictions which allows us to disentangle the atomic parentage of each photoemission band. This assignment helps to explain the energy and intensity changes detected experimentally in passing from synchrotron to XPS spectra. The origin of the outer valence bands B and A has been discussed in detail since much controversy exists in recent works concerning the atomic composition of these bands. Band B has been clearly shown to involve both nitrogen lone pairs and C_{2p} π-electronic levels, while band A is demonstrated to result exclusively from the highest occupied valence band originating in the C_{2p} $4a_u$ π orbitals of the phthalocyanine molecules.

Acknowledgment. We thank the CIUV (Centro de Informàtica de la Universitat de València) for the use of their computing facilities. The work in Valencia has been partly supported by the DGICYT Projects PS88-0112 and OP90-0042 and that in Mons by the Belgian "Pôle d'Attraction Interuniversitaire en Chimie Supramolèculaire et Catalyse".

---

(71) Von Niessen, W.; Kraemer, W. P.; Diercksen, G. H. F. *Chem. Phys.* **1973**, *41*, 113.

(72) Almlöf, J. *Int. J. Quantum Chem.* **1974**, *8*, 915. Christoffersen, R. E. *Ibid.* **1979**, *16*, 573. Nagashima, U.; Takada, T.; Ohno, K. *J. Chem. Phys.* **1986**, *85*, 4524.

(73) Ortí, E.; Brédas, J. L. *Chem. Phys. Lett.* **1989**, *164*, 247.